SURFACE SHAPE MEASUREMENT AND EVALUATION OF MECHANICAL STABILITY BY DEM SIMULATION FOR DAMAGED TRADITIONAL STONEWALLS

*Satoshi Sugimoto[1], Maho Yamaguchi[1] and Minoru Yamanaka[2]

[1]Faculty of Engineering, Nagasaki University, Japan; [2]Faculty of Engineering, Kagawa University, Japan

ABSTRACT: Kumamoto Castle has constructed about 400 years ago, and now the Cultural Affairs Agency of Japan treats it as an important historical spot. The 2016 Kumamoto Earthquake was damaged a lot of stone walls of this castle. Authors continue to investigate the deformation of unstable stonewalls by high accuracy laser module for measuring distance. And these stonewalls should be monitored continuously for evaluation of mechanical stability, so we developed and established the wireless network system for measuring the changing angle of some stonewalls surface in this castle. When installing this system in the future, the results of shape measurement of the surface of these stone walls will be important in identifying the locations to be installed and setting priorities. The authors also carried out making a simulation model and calculation for evaluation of stonewalls stability by the distinct element method under the several conditions of stonewall shape and interface of materials. The failure area of stone walls and backfill are estimated by these results of DEM simulation, and it is discussed that these areas should be reinforced under the repair of damaged stonewalls.

Keywords: Damaged stone wall, Stability, Surface shape and DEM simulation

1. INTRODUCTION

The 2016 Kumamoto earthquake caused enormous damage to ground structures such as buildings and stone walls at Kumamoto Castle. Besides, many stone walls in Kumamoto Castle collapsed and overturned, and tensile cracks occurred in the back of the embankment. The 2016 Kumamoto earthquake is characterized by the fact that Kumamoto Castle was damaged by a foreshock with a seismic intensity of 5+ and the main shock of 6+. Although the stonewalls of Kumamoto Castle escaped deformation during the foreshock, many cases were found to have been deformed or collapsed due to the mainshock [1,2]. And the stone walls that have undergone deformation will be examined for restoration work and appropriate management in the future. However, it is very difficult to distinguish whether the stone wall originally had a deformation or if the deformation was caused by the earthquake. Therefore, when considering the priority of restoration from the degree of deformation, it is required for the administrator to perform simple measurements daily. Besides, it is necessary to elucidate the mechanism of the stone wall collapse so that similar damage will never occur again in the future when another large-scale earthquake will occur. In this study, we used a simple method to quantitatively measure the deformation of the stonewall and used data collection and the distinct element method (analysis code: UDEC) to support the selection of remote monitoring points [3,4]. Based on the research, we will build a model of stone walls. Then, numerical analysis of dynamic behavior was carried out, and factors affecting the stone wall were examined by comparing the collapse patterns under various conditions.

2. TYPE OF STONEWALL STRUCTURE

The stone walls of Kumamoto Castle can be roughly divided into three types according to the internal structure of the stone walls. In this study, the three types of shapes were named "stone base type", "half stone base type", and "stoneless base type" by adding the distance to the literature [5-7]. Figure 1 shows the three types of internal structure, shape characteristics, and constituent materials. The stone base type is a stone wall with a low height, so many are made around the gate. The half stone base type is often made in the stone walls around the moat or the main enclosure. Since the northwestern part is not along the mountains, it is thought that many stone walls on this side were made of soil embankments and rubble. Many stoneless base types are made from south to southeast of Kumamoto Castle. This is probably because it was possible to pile up stonewalls on a steep slope. After all, the southeast side is along Mt. Chausu.

3. MEASUREMENT WITH A PORTABLE LASER RANGEFINDER

The Leica Geosystem's DISTO D510 is a portable laser rangefinder that is mainly used to measure the shape of land plots and buildings. As shown in Figure 2, it is easy to measure linear distances and elevation angles. This instrument has an accuracy of 1.0 mm per 10 m and is available at a measuring distance of up to 200 m. Furthermore, it has been shown that there is a variation of about 0.3% when the angle between the measuring instrument and the horizontal plane exceeds 45 degrees. Therefore, in this study, it is necessary to fix the portable laser range finder (DISTO D510) to a tripod, measure the vertical distance and the horizontal distance, and to measure the shape within the range of 45 degrees. The condition was set.

Type name	Stone base type	Half stone base type	Stoneless base type
Style			
State at the time of collapse			
Materials	Stone Cobblestone	Stone Cobblestone Embankment	Stone Embankment
Height	Low	A little high	High
Slope	steep	A little lenient	A little lenient

Fig. 1   Shape features of each stonewall

3.1 Measuring Method

The measurement was performed according to the following procedure. Install a measure parallel to the surface of the stone wall to be measured. At this time, either the left or right end is set as the measurement origin. A marker is set at the point set as the origin so that it can be easily compared in future measurements. Determine the distance between survey lines according to the length and size of the stone wall. After determining the measuring line, install the measure so that it intersects with the measure installed parallel to the stone wall. Install a portable laser range finder (DISTO D510) on the tripod and measure the measurement point. At this time, one point will be measured for each stone wall on the survey line, and the center of the stone wall will be measured.

There are two ways to organize the data in the measured stone wall cross-section: top reference and bottom reference.

The top reference is the uppermost stonewall as the origin of the X-axis and the Y-axis, and the bottom reference is the measured data with the lowermost stone wall as the X-axis and the Y-axis origin. By setting a standard, it is easy to judge the characteristics of the deformation and collapse of the stone wall when the surface shape of the stone wall changes. Moreover, based on the bottom of the

stone wall, the measured lateral position, height, and depth were input into the graph drawing software to create a shape distribution map. As shown in Fig. 2, a laser range finder fixed on a tripod is installed in front of the target stonewall, and the distance and angle of each stone wall are measured in the vertical direction. After the measurement, find the vertical and horizontal coordinates of each stone wall based on the distance and angle and plot the cross-section. If the ground where the stone wall is built inclines, it is difficult to create an accurate surface shape distribution map if measured normally. Therefore, when performing the measurement, we decided to use the bottom of the slope as the origin of the coordinate axis and use the two poles to measure the step. The distance between poles can be found by using two poles. Therefore, by adding the vertical distance between poles to each survey line, the standard can be unified and a surface shape distribution map can be created. Photo 1 shows the measurement using a pole.
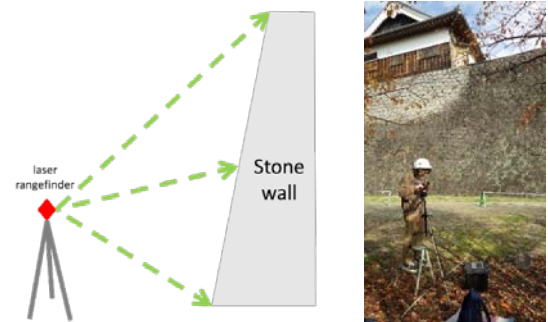
Fig. 2   Measurement schematic diagram and photo

Photo 1   State of pole installation

4. SURFACE SHAPE MEASUREMENT

A portable laser range finder was installed in front of the target stone wall, and the distance and angle of each stone wall were measured in the vertical direction. After the measurement, the vertical and horizontal coordinates of each stone wall were calculated based on the distance and angle, and the cross-section was plotted. This time, the measured data of 1984 and 2018 were used for comparison. The 1984 data is the newest data measured by Prof. Kuwahara [8] before the Kumamoto earthquake. In selecting the measurement points, in addition to the points measured in the past, we newly measured the points with large deformation. Up to now, the measurement has been performed in 8 steps, and a total of 150 points have been measured as shown in Fig. 3.
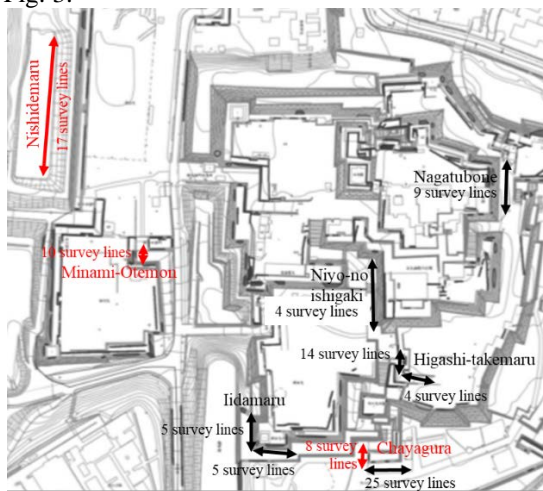

Fig. 3   Overall view of measurement points

4.1 Stonewall of "Chayagura" Trace

It is a stone wall located on the south side of Kumamoto Castle. Photo 2 is a panoramic view of the western surface of the stone wall at "Chayagura" trace. A total of 8 lines were measured at 1m intervals. Figure 4 shows the surface shape distribution map of the western surface of the stonewall. At around 5m, the surface shape is protruding. The possible reason for this is considered to be a phenomenon caused by the reduction of the gap between the stones, which is caused by the movement of the stones accumulated in the rear part of the stone wall due to the influence of external force such as vibration. It was confirmed at the site that the deformed parts were the same with this figure. This deformation seems to reflect the result of active earth pressure in the central part of the stone wall during the earthquake.
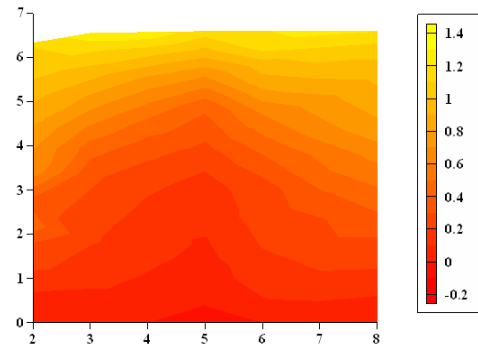

Photo 2   Stonewall of "Chayagura" trace

Fig. 4   Surface shape distribution map (unit: m)

4.2 Stone Wall of "Nishide-maru"

It is a stone wall located in the northwest of Kumamoto Castle. A total of 17 lines were measured at 5m intervals. Due to the Kumamoto earthquake, there are some places where the stone wall collapsed as shown in Photo 3. As shown in Figure 5, some ridges are seen near the bottom of the stonewall, but they tend to be different from the deformations seen in other stone walls, so it is thought that the effects of consolidation settlement of the foundation and active soil pressure on the back ground are high.
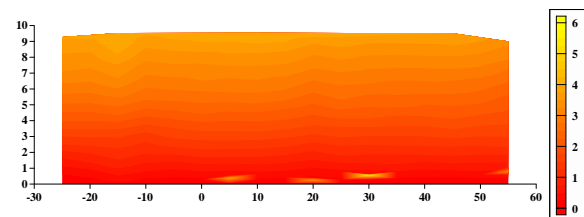

Photo 3   Stone wall of "Nishide-maru"

Fig. 5   Surface shape distribution map (unit: m)

4.3 Stone Wall of "Minami-Otemon"

The stone wall of Minami-Otemon is a stone wall with a cobblestone on the back, and it is presumed that it was affected by the earthquake. Due to the effects of post-earthquake construction, it was not possible to make measurements at this point. A full view of stone wall is shown in Photo 4. The surface shape measurement was based on the bottom of the left end, and rightward and upward were positive. In addition, the distance between the survey lines was 1 m, and a total of 10 survey lines were measured. As shown in Figure 6, some overhang was observed in the central part of the stonewall around 5 to 9 m. At this point, the same tendency of deformation as that of the stone wall of Chayagura trace was confirmed.

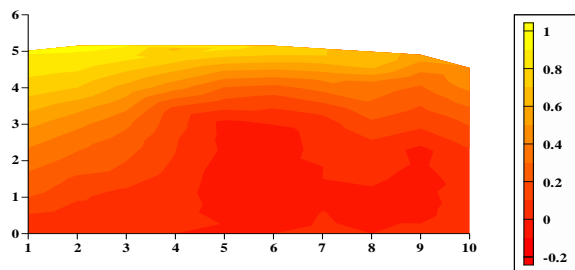Photo 4　Stone wall of "Minami-Otemon"

Fig. 6　Surface shape distribution map (unit: m)

5. DYNAMIC ANALYSIS BY DISTINCT ELEMENT METHOD

The stone base type among the three types of stone walls was modeled by the distinct element method program (analysis code: UDEC) and the dynamic analysis was performed. In this research, the distinct element method (analysis code: UDEC), which is suitable for analyzing discontinuous structures such as stone walls and stone bridges, is used to reproduce individual movements of stone walls and stones. The stone base type consists only of chestnut stone and stone wall stone, and the damage was the largest of the three types, and more than half of the total collapsed, so this paper describes the results of this type.

5.1 Analysis Model

Figure 7 shows a "stone base type" analytical model with a stonewall slope of 70°. Since the stone base type is built in a place where there is no background, stones were piled up on the left and right, and the inside was packed with a quarry stone block, as in the previous literature. The sandy ground represented by elasto-plastic elements was installed under the stone wall, and in the actual stone wall, the lower stone wall was buried in the ground, so the lower three steps were fixed as the foundation.

5.2 Boundary Condition

In this study, the boundary conditions shown in Figure 7 were set to properly reproduce the transmission of seismic waves from deep underground. A dashpot was provided on the boundary surface of the sandy ground at the bottom of the individual element model to make the bottom viscous boundary. The bottom viscous boundary is a boundary condition that evaluates the semi-infinite ground below the model bottom, and it is possible to absorb the wave energy dissipated at the bottom boundary and input only the rising wave component of the seismic wave. As a result, the transmission characteristics of seismic waves from deep underground can be satisfied. A free rock mass region was set up on both boundary surfaces on the side of the distinct element method model as energy transfer boundaries. The energy transfer boundaries allow wave energy to be dissipated laterally in the model and absorbed in the free rock region. As a result, the lateral boundary can be evaluated as a semi-infinite ground area, and the actual foundation rock area can be reproduced [9].
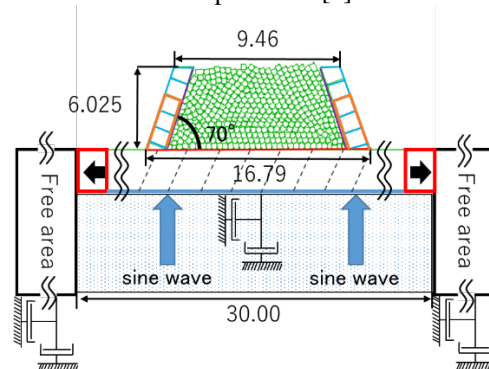
Fig. 7　Cross-section of the analysis model (unit: m)

5.3 Input Parameter

Table 1 shows the characteristic values of the surface of each block, and Table 2 shows the characteristic values of each joint. In this study, we focused on the stone base type that caused the most

damage. To compare with the existing literature, the characteristic value was analyzed with the same value as the previous research. And the density of stones and cobblestones are applied each 2.5 kg/cm^3 and 2.2 kg/cm^3.

5.4 Model Creation

Figure 7 shows a drawing of the stone base type with a stonewall slope of 70°. The left figure is a model before cutting the stone. We made two blocks inside the stonewall and one block above the stone wall and cut the block into 40 cm square. Since it is harder to create a gap when dropping one block than dropping it separately, we created blocks separately. In order to get closer to the actual construction procedure, rubble stones were made at a certain height and allowed to fall freely and packed inside the stonewall. Based on the reflections of previous studies, a gap was created in the corner of the stonewall just by free fall, so acceleration was applied in any direction to the model with the stone wall and the base fixed. From this, as shown in Figure 8, it can be confirmed that the stones are sufficiently clogged.
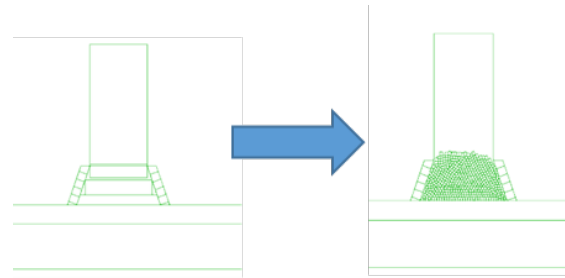
5.5 Earthquake Motion Input

The input ground motion is given to the bottom of the individual element model. The input waveform had a frequency of 10 Hz, an amplitude of 1 m/sec, and an excitation time of 2 seconds, after which the gravity analysis was performed for 1 second [10].

Table 1   Characteristic value of block surface

	Case 1	Case 2
Normal stiffness (N/mm)	3000	3000
Shear stiffness (N/mm)	3000	3000
Cohesion (kN/m²)	0	0
Shear resistance angle (deg)	15	30

Table 2   Shear resistance angle value between different materials

Stones and cobblestones (deg)	Stones and sandy ground (deg)	Cobblestones and sandy ground (deg)
15	15	15
Stones and cobblestones (deg)	Stones and sandy ground (deg)	Cobblestones and sandy ground (deg)
15	15	15

Fig. 8   Schematic diagram of the stone base type model creation

5.6 Relationship between Stone Wall Height and Collapse Range

In order to clarify the relationship between the height of the stone wall and the collapse range, the condition of the physical properties of each block was not changed, and only the height was set to half the value of the previous studies. The height of the stonewall used in the previous research is 12.0 m, and the height of the stone wall used in this research is 6.0 m. Figure 9 shows the analytical model of 12.0m and 6.0 m with a shear resistance angle of 15° on the surface of each block with a stone wall slope of 70°.

Figure 10 shows the displacement vectors of the 12.0 m high model and 6.0 m high model during deformation. As the height of the stone wall became lower, a difference appeared in how it collapsed under the same conditions. The slope of the slip surface varies depending on the height of the stone wall. This is because when the height is 12.0 m, the earth wall pressure is relatively small and the earth cover pressure is relatively small. Therefore, the horizontal force acting by the inertial force of the seismic motion is larger than the earth's cover pressure. It is considered that the surface inclination is steep. When the height is 6.0 m, the height of the stone wall is low, so the force exerted by the overburden pressure does not change much depending on the place, and the horizontal force acting by the earthquake motion is larger than the overburden pressure. It is considered that the slope of the slip surface is gentle.

Figure 11 shows a comparison of the horizontal displacement of the stone wall at the top of the crown when a ground motion is applied, based on the height. When the height was 12 m, the horizontal displacement was larger than that when the height was 6 m. In both cases, although the stone wall has collapsed, the height of the stone wall is higher than that of the lower stone because it is taller, and it is thought that the stone wall was more susceptible to the influence of the stone. In addition, it is considered that the movement of the upper area also differs depending on how the clogs are clogged.
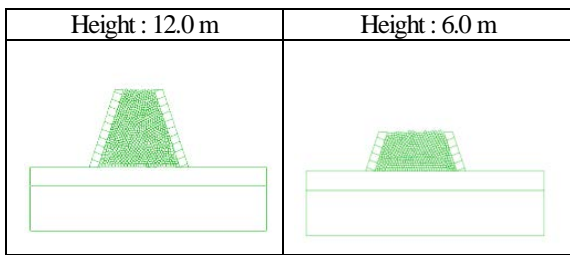
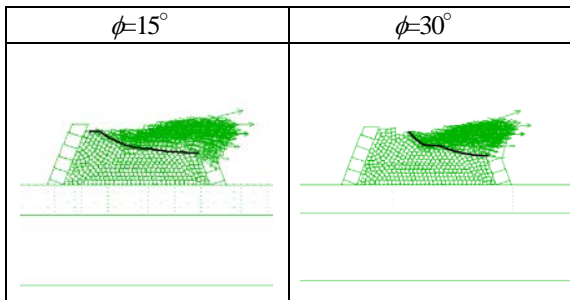Fig. 9   Two kinds of models of stonewalls

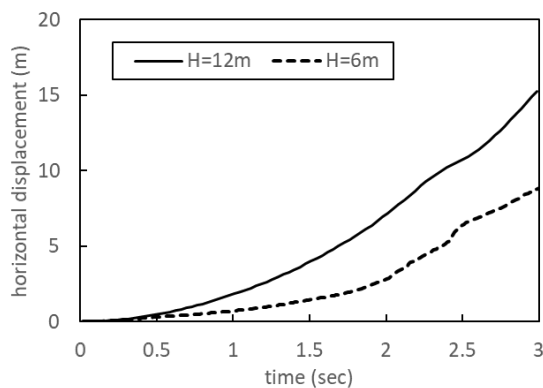Fig. 10   Displacement vector diagram after the start of earthquake motion

Fig. 11   Horizontal displacement of the top of the stonewall compared with height

5.7 Relationship Between Shear Resistance Angle And Collapse Range

In order to clarify the effect of the size of the shear resistance angle on the cobblestone surface on the collapse of the stone wall, the other parameters were constant, the stone wall slope was 70°, the height was 6.0 m, and the shear resistance value of each block was The calculation was performed under the conditions of 30° and 15°. The results are shown in Figure 12. When Case 1 and Case 2 are compared, the inclination of the slip surface is significantly different because the shear resistance angle is different even if the height is the same. The distinct element method was used to express that the larger the shear resistance angle, the more difficult the stone wall is to collapse.

Figure 13 shows a comparison of the horizontal displacement of the stonewall at the top of the crown when a ground motion is applied, based on

the value of the shear resistance angle. When the shear resistance angle is 15°, the upper stone wall is displaced from 0.25 seconds after the start of vibration, whereas when the shear resistance angle is 30°, the vibration is observed from 1.75 seconds after the start of vibration. It is considered that the larger the shear resistance angle is, the larger the force to resist when the earthquake motion is applied becomes, and it becomes difficult to transmit the force to the upper stone wall.
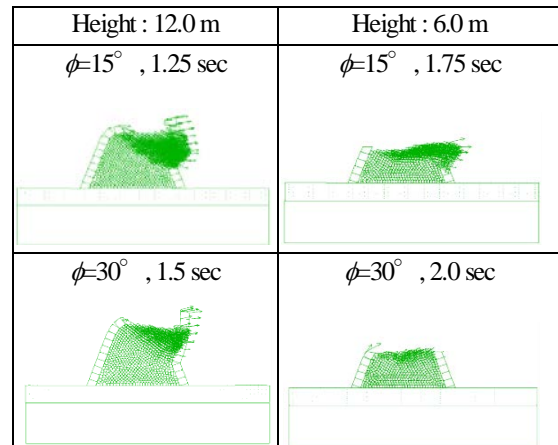

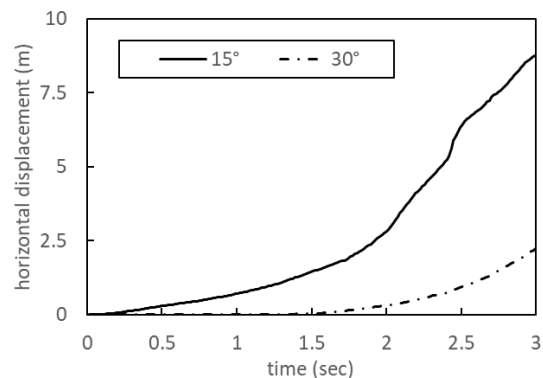Fig. 12   Slip surface compared with each shear resistance angle

Fig.13   The horizontal displacement of the top of the stonewall is compared with the shear resistance angle.

6. CONCLUSION

In this study, the simple method is used to quantitatively measure the deformation of the stone wall, data collection and stone base type stone wall are used as the basis for the selection of the remote monitoring target, and the distinct element method (A dynamic analysis was performed using the analysis code: UDEC) to reproduce the collapse behavior of the stone wall. The results and considerations obtained in this study are described below.

1) Using a portable laser rangefinder, the surface shape of stone walls at various places in Kumamoto

Castle was measured easily. In the stone wall with a height of about 5 m, many deformations were observed, which seemed to be extruded by the stones on the back. It is highly probable that a temporary active earth pressure condition was caused by the earthquake motion. Although it is necessary to verify the consistency with the 3D measurement results, it is a simple measurement method, but it is possible to quantitatively grasp the characteristics of the surface shape.

2) The damage situation at each height of the stone wall was collapsed in all cases when the height was 12 m. On the other hand, when the height was halved to 6 m, no collapse occurred when the shear resistance angle of the stonewall and the stone was 30°. From this, it can be confirmed that not only the slope of the stone wall but also the height of the stone wall contribute to the collapse.

3) It was found that the higher the height of the stone wall, the greater the depth of the stone, and the lower the height, the gentler the slope of the slip surface.

4) It was found that the stone-base type collapse factor in which the stone is composed is the active earth pressure generated when the stone is destroyed by the earthquake. However, it was confirmed that if the shear resistance angle of the stones exceeds a certain value, the active earth pressure is not generated enough to collapse the stone wall.

5) Even with the same height model, if the shear resistance angle is different, the displacement of the stone wall in the upper stage when vibration is applied is different. It is thought that this is because the larger the shear resistance angle, the greater the force that tries to resist when an earthquake motion is applied, and the more difficult it is to reach the upper stonewall.

7. ACKNOWLEDGMENTS

8. REFERENCES

[1] Sugimoto S., Yamanaka M., Maeda H., Fukuda N., Katsuda Y.: Research of damaged condition by the 2016 Kumamoto Earthquake and ground investigation on stone walls and earth structures in Kumamoto Castle, International Journal of GEOMATE, Vol.14, Issue 45, 2018, pp.66-72.

[2] Sugimoto S., Yamanaka M.: Reports of damaged earth structures in Kumamoto Castle, Proceedings of 54th Natural disaster and science symposium, 2017, pp.45-51. (in Japanese)

[3] Katsuda Y., Jiang Y., Omine K., Sugimoto S.: Research of damaged stone structures in Kumamoto Castle by the 2016 Kumamoto Earthquake, Proceedings of 72th JSCE Conference (CD-ROM), 2017, pp.479-480. (in Japanese)

[4] Katsuda Y., Sugimoto S., Yamanaka M.: Reports of a survey on damaged stonewalls in Kumamoto Castle by the 2016 Kumamoto Earthquake, Proceedings of the Japan National Conference on Geotechnical Engineering, 2018. (in Japanese)

[5] Yamamoto H., Nishigata T., Yao S., Nishida K., Kasa H., Wada I.: Study on Friction Characteristics of Stones and Effect of Packing in Castle Stone Wall, Proceedings of the National Symposium on Ground Improvement, 2008, pp.127-132. (in Japanese)

[6] Nishimura T., Noma Y., Kasa H., Yamamoto H., Nishigata T.: Examination of deformation behavior of shaking table test by stability analysis of castle wall using distinct element method, Proceedings of 66th JSCE Conference (CD-ROM), 2011, pp.325-326. (in Japanese)

[7] Kasa H., Yamamoto H., Awatani T., Nishida K., Nishigata T., Wada Y.: Experimental study on stability improvement effect of boulder stone in the castle wall, Proceedings of 62th JSCE Conference (CD-ROM), 2007, pp.467-468. (in Japanese)

[8] Kuwahara F..: The gradient of the stone walls in Kumamoto Castle, Report of researches / Nippon Institute of Technology, 14-2, 1984, pp.59-74. (in Japanese)

[9] Fujii I., Yang L., Jiang Y., Li S., Tanahashi T.: Evaluation of the dynamic behaviors of the bedrock containing discontinuities under important buildings based on numerical simulations, Proceedings of 2011 JSCE west conference (CD-ROM), 2011, pp.411-422(in Japanese)

[10] National Research Institute for Earth and Disaster Resilience "K-NET", http:www.kyoshin.bosai.go.jp/kyoshin/,2017.